

Mapping Transition-edge Sensor Temperature Sensitivity and Current Sensitivity Surface as a Function of Current, Magnetic Field and Temperature with IV curve and Complex Impedance Measurement

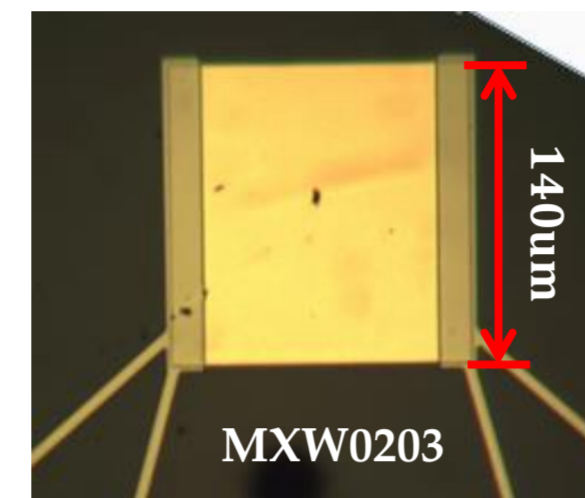
Yu Zhou, Felix. T. Jaeckel, Dan McCammon, Kari. L. Kripps, Shuo Zhang, Rachel Gruenke, Dallas Wulf, C. V. Ambarish, K. M. Morgan*
 Physics Department, University of Wisconsin – Madison, Madison, WI, USA
 J. S. Adams, S. R. Bandler, J. A. Chervenak, A. M. Datesman, M. E. Eckart, A. J. Ewin, F. M. Finkbeiner,
 R. L. Kelley, C. A. Kilbourne, A. R. Miniussi, F. S. Porter, J. E. Sadleir, K. Sakai, S. J. Smith, N. A. Wakeham, E. J. Wassell, W. Yoon
 NASA Goddard Space Flight Center, Greenbelt, MD, USA

Motivation

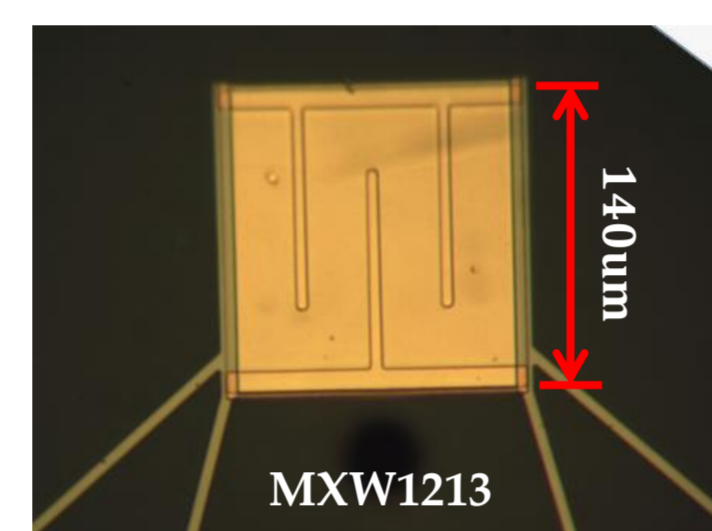
1. To resolve the spectra of the astronomical diffuse X-ray background in the 0.1-0.5 keV energy range, we need large area pixels (~1mm²) with excellent energy resolution (1-2 eV).
2. For TES pixels with large absorbers that have a relatively high heat capacity, high α and low β are needed to achieve the required energy resolution.
3. Most work in the field has found high α to be correlated with high β and also with excess noise. The cause of this correlation remains to be understood[6].

TES devices – overview^[5]

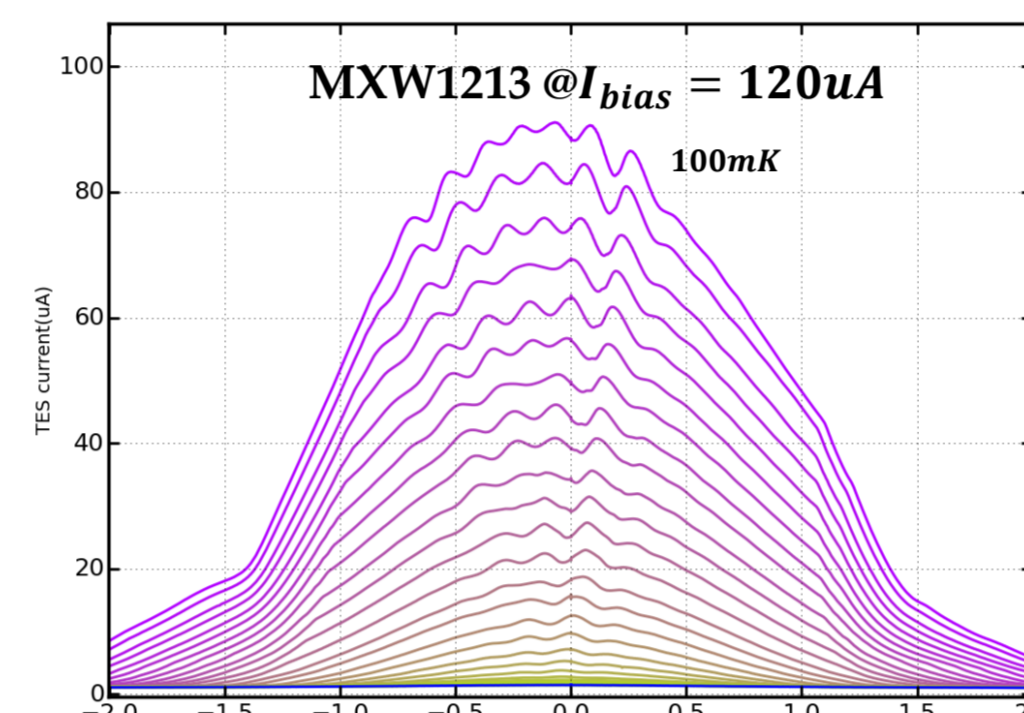
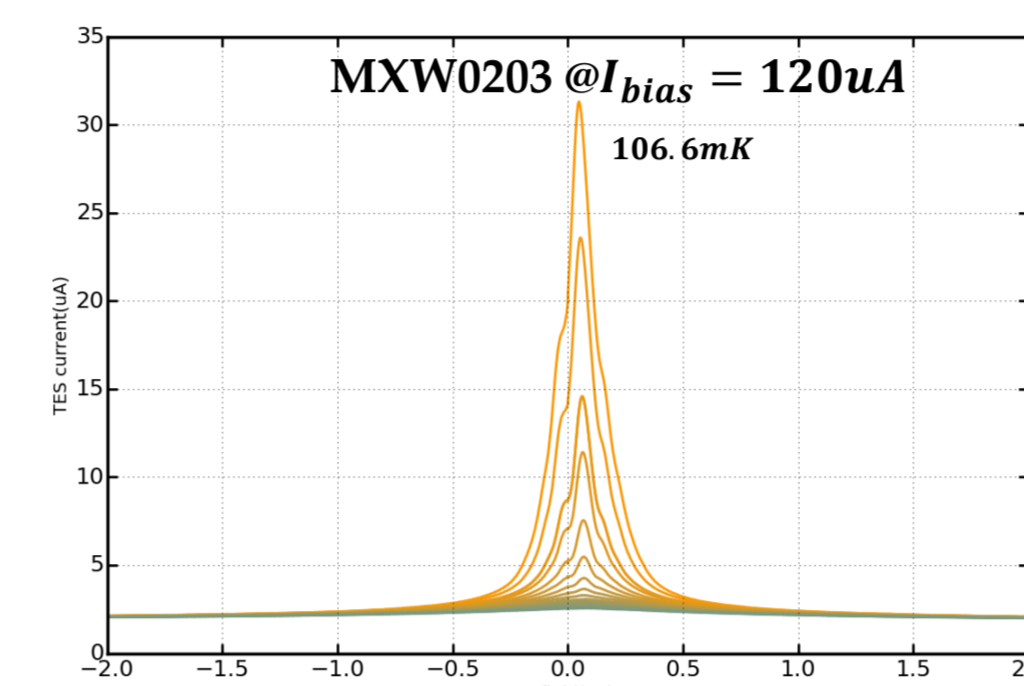
- ◆ Mo-Au bilayer
- ◆ No membrane/absorber



No zebra strips or banks



3 strips with banks

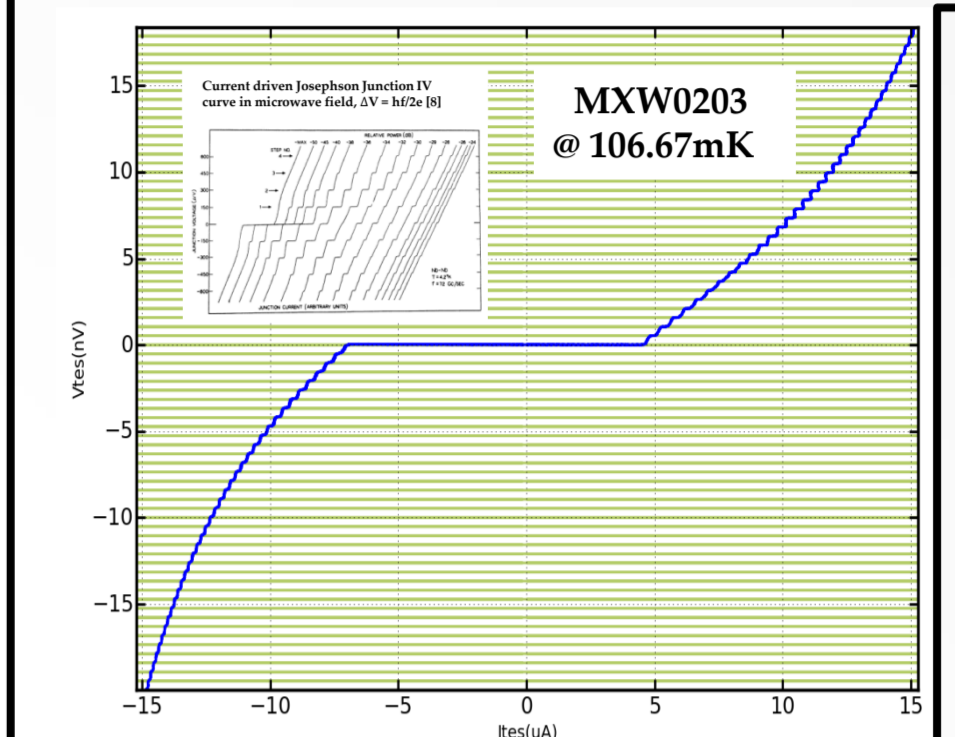


These two Mo-Au bilayer TESs are diagnosis chips with no membrane or absorber design. MXW0203 T_c ~ 108mK; MXW1213 T_c ~ 104mK. Here we take I_{TES} vs. B_{ext} for two devices at different temperature.

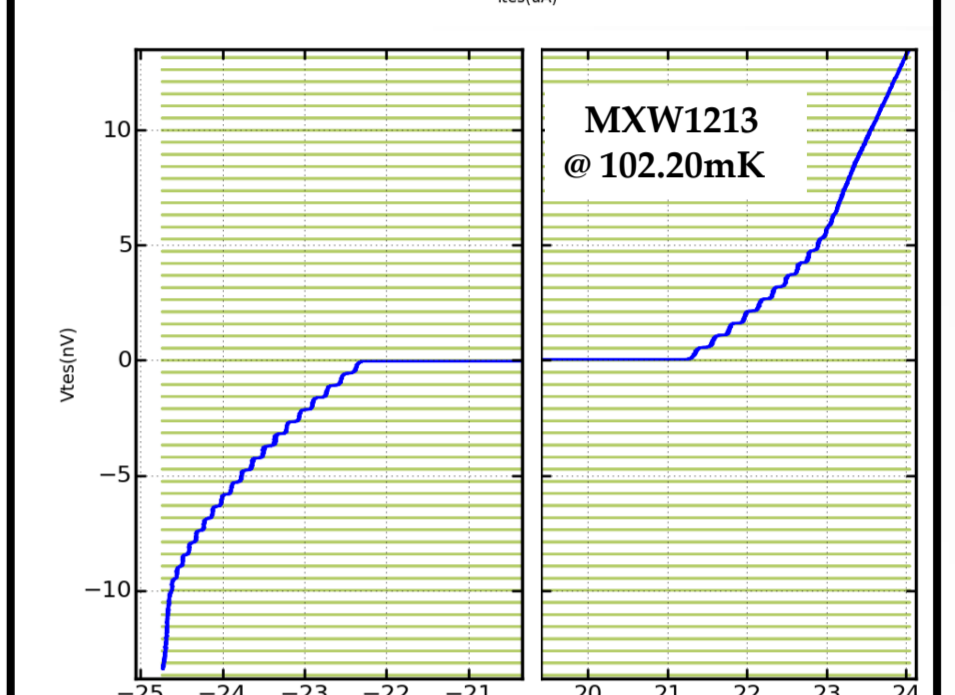
MXW0203: I_{bias} = 120uA Bath Temperature ranging from 106.6mK to 109.6mK, in steps of 0.2mK

MXW1213: I_{bias} = 120uA Bath Temperature ranging from 100.0mK to 105.4mK, in steps of 0.2mK

TES behaves like a Josephson Junction (Shapiro Steps)[7]



MXW0203–IV curve taken at 106.67mK. An external alternating B-field is applied to the device. Frequency = 254.276kHz



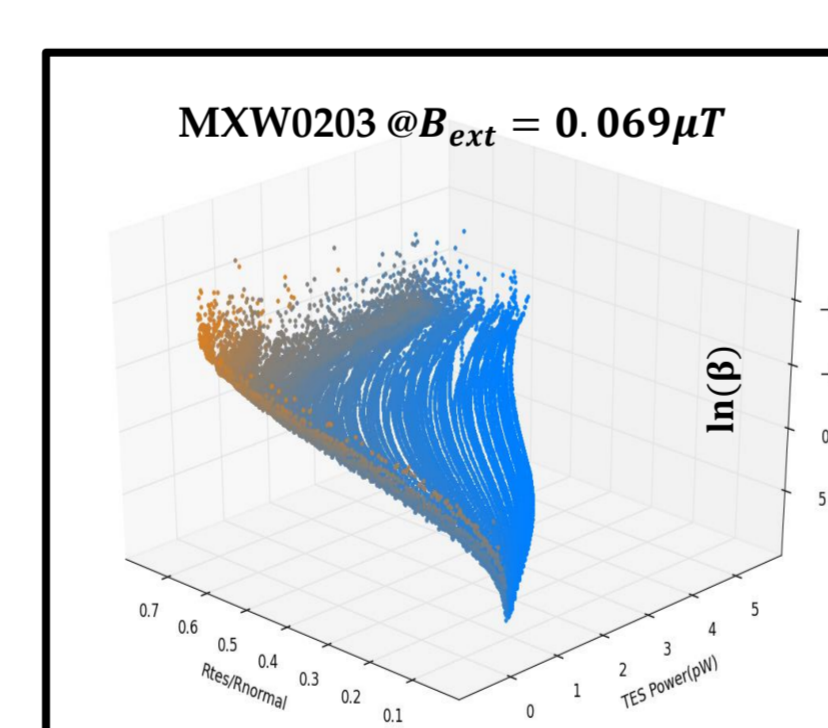
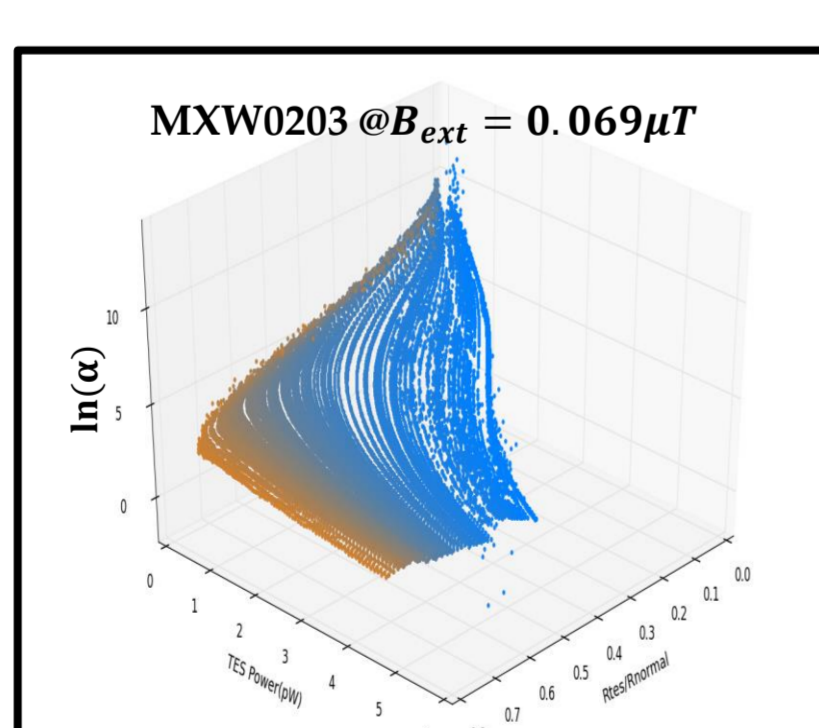
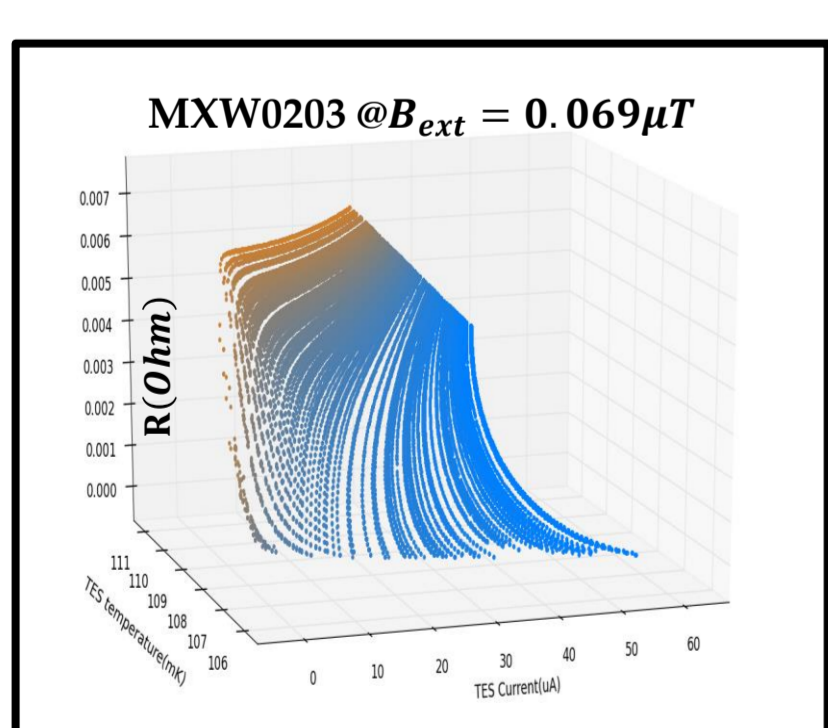
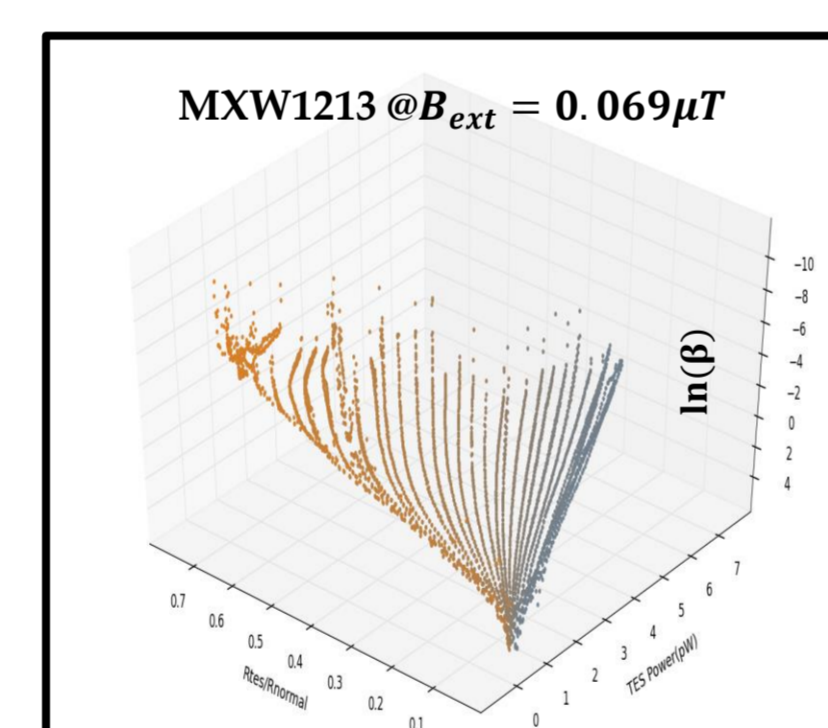
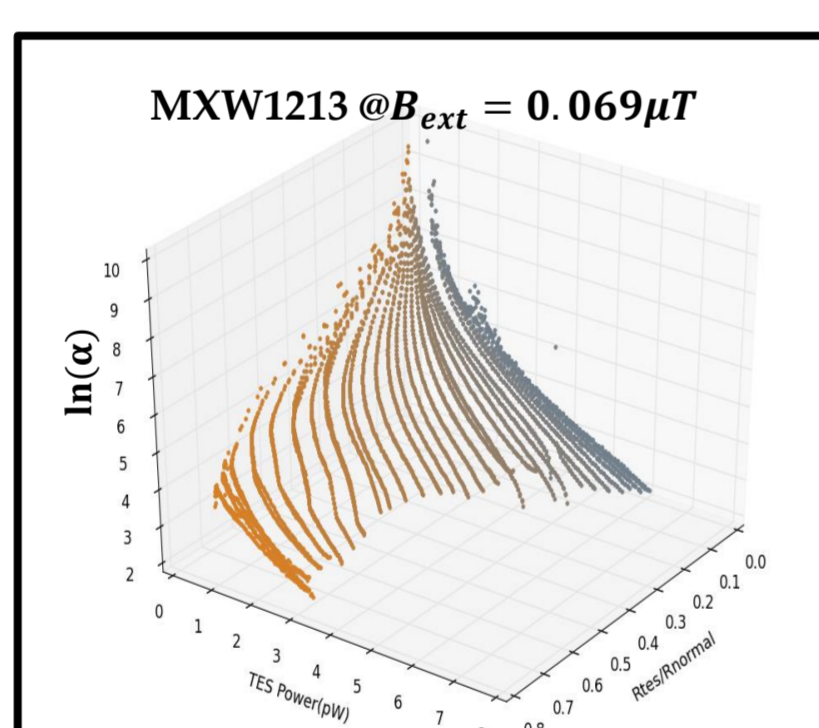
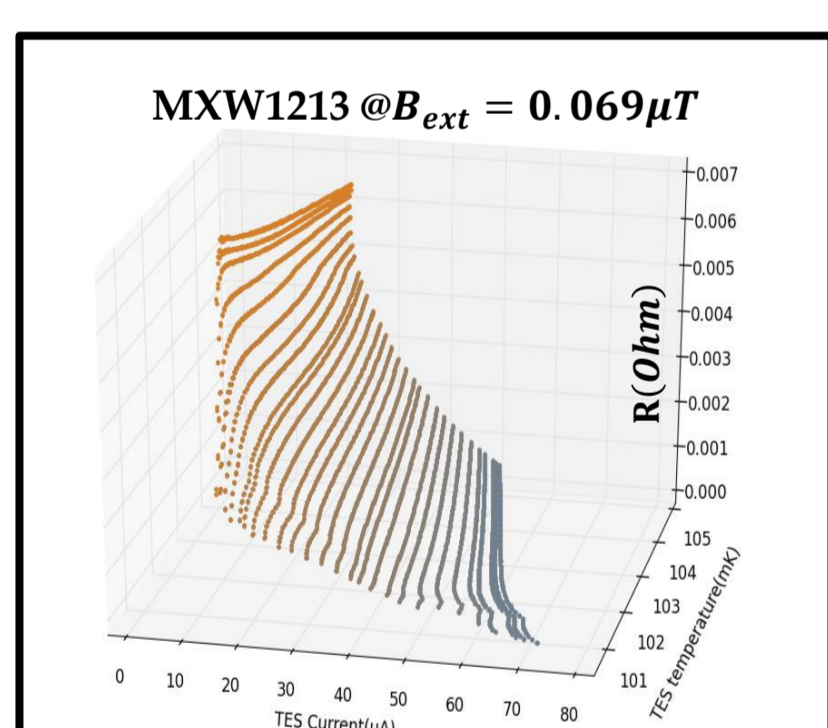
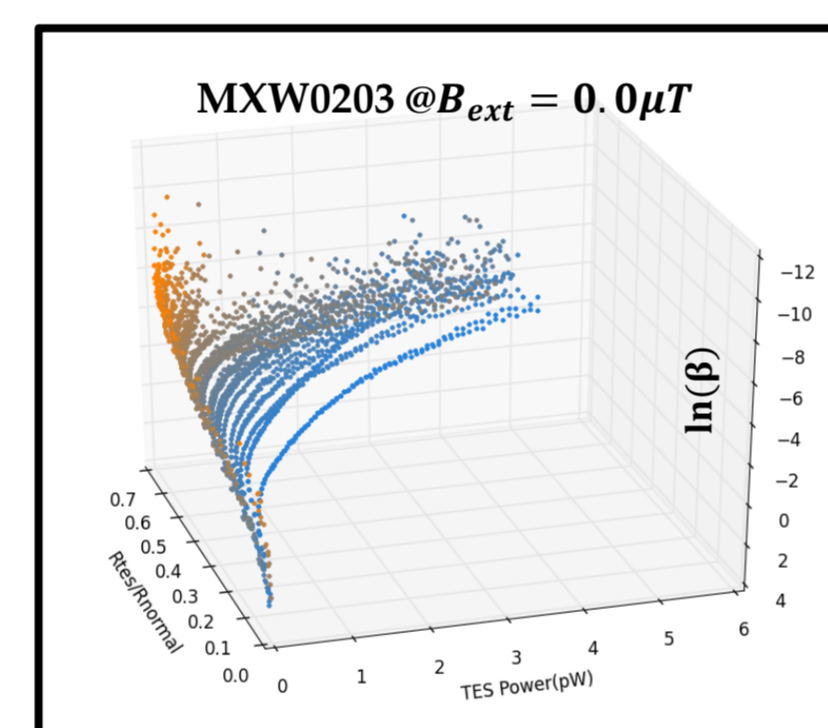
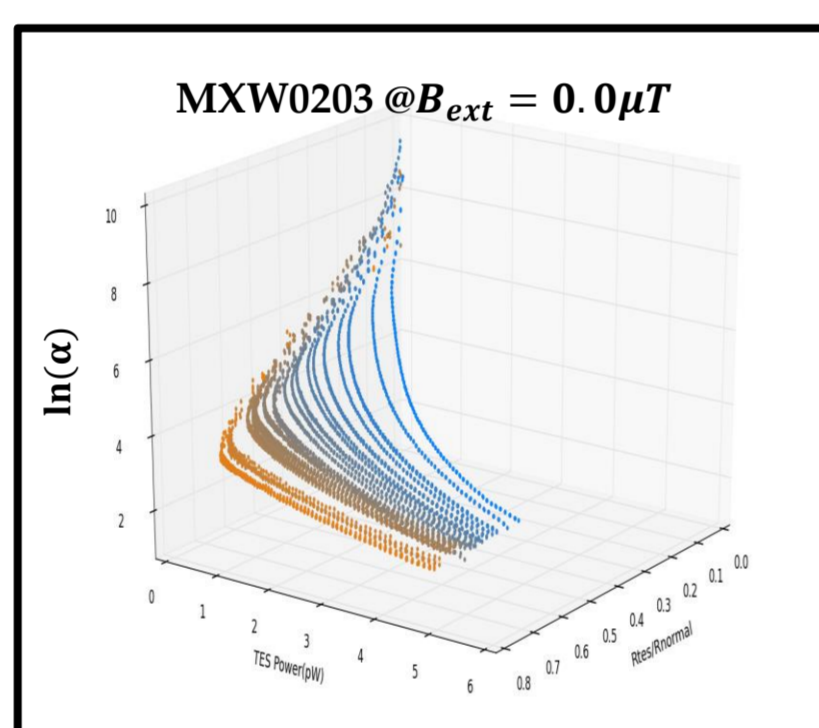
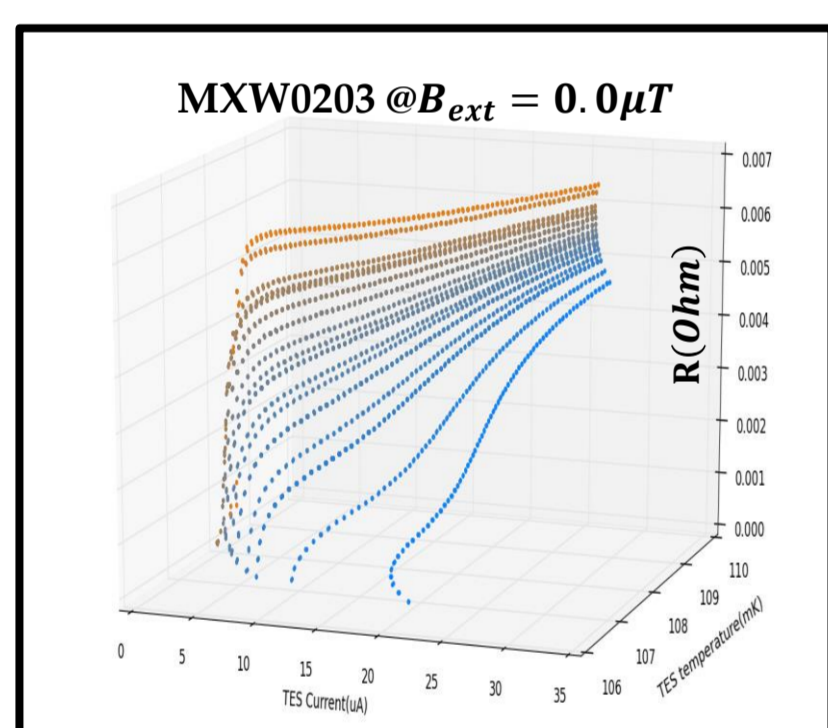
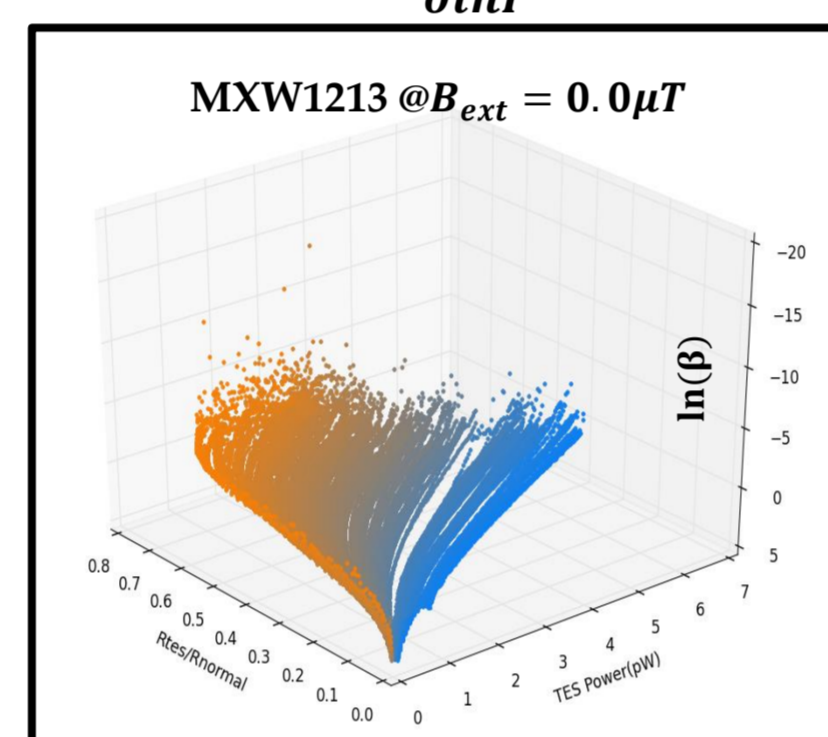
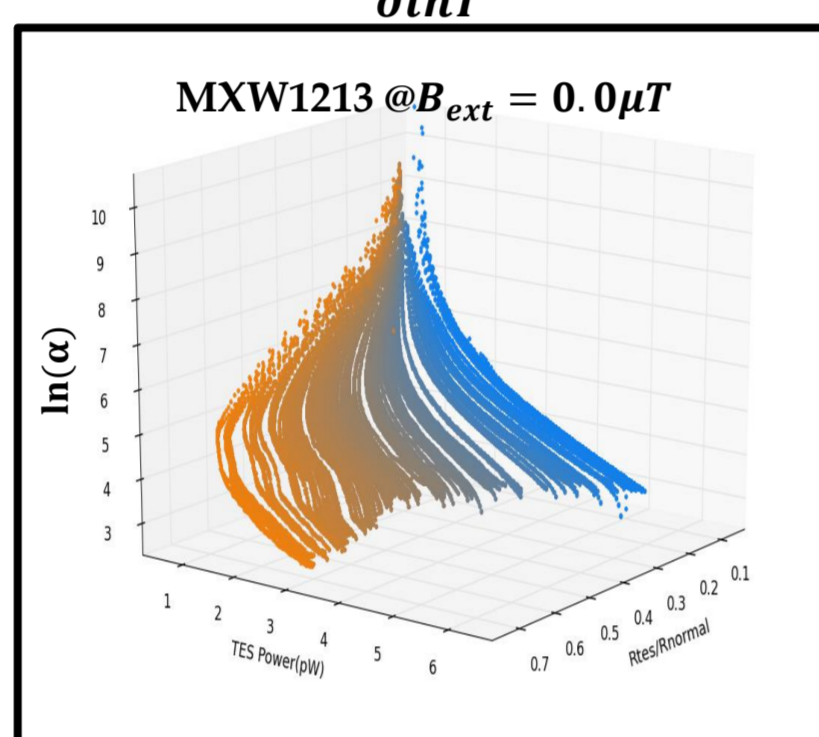
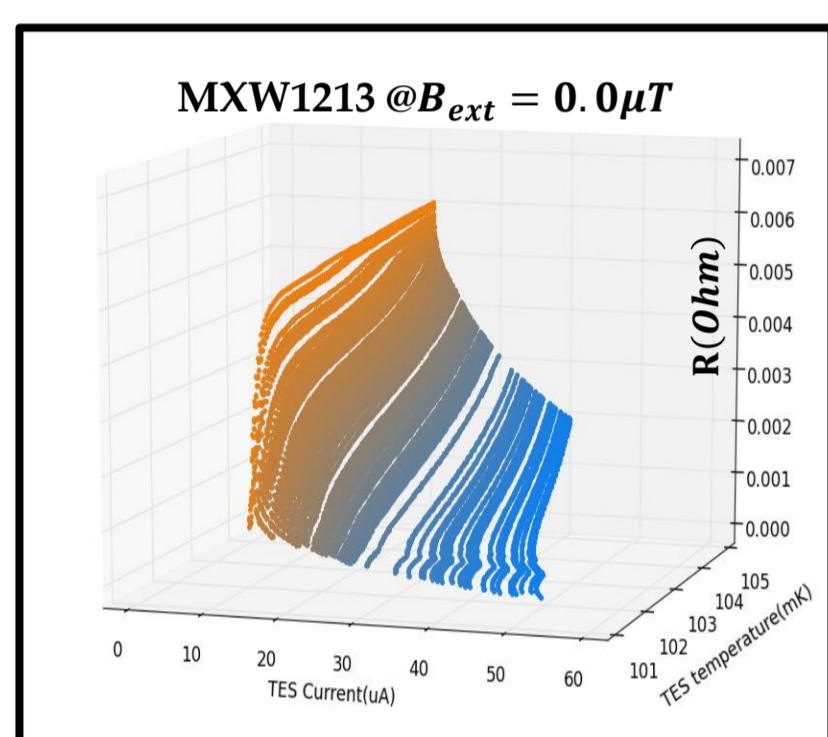
MXW1213–IV curve taken at 102.20mK. An external alternating B-field is applied to the device. Frequency = 254.276kHz

With $\Delta V_{TES} = 4\mu V$, we were able to calibrate the shunt resistance to a precision of 1 $\mu\Omega$.

R(I, T)

$$\alpha = \frac{\partial \ln R}{\partial \ln T}$$

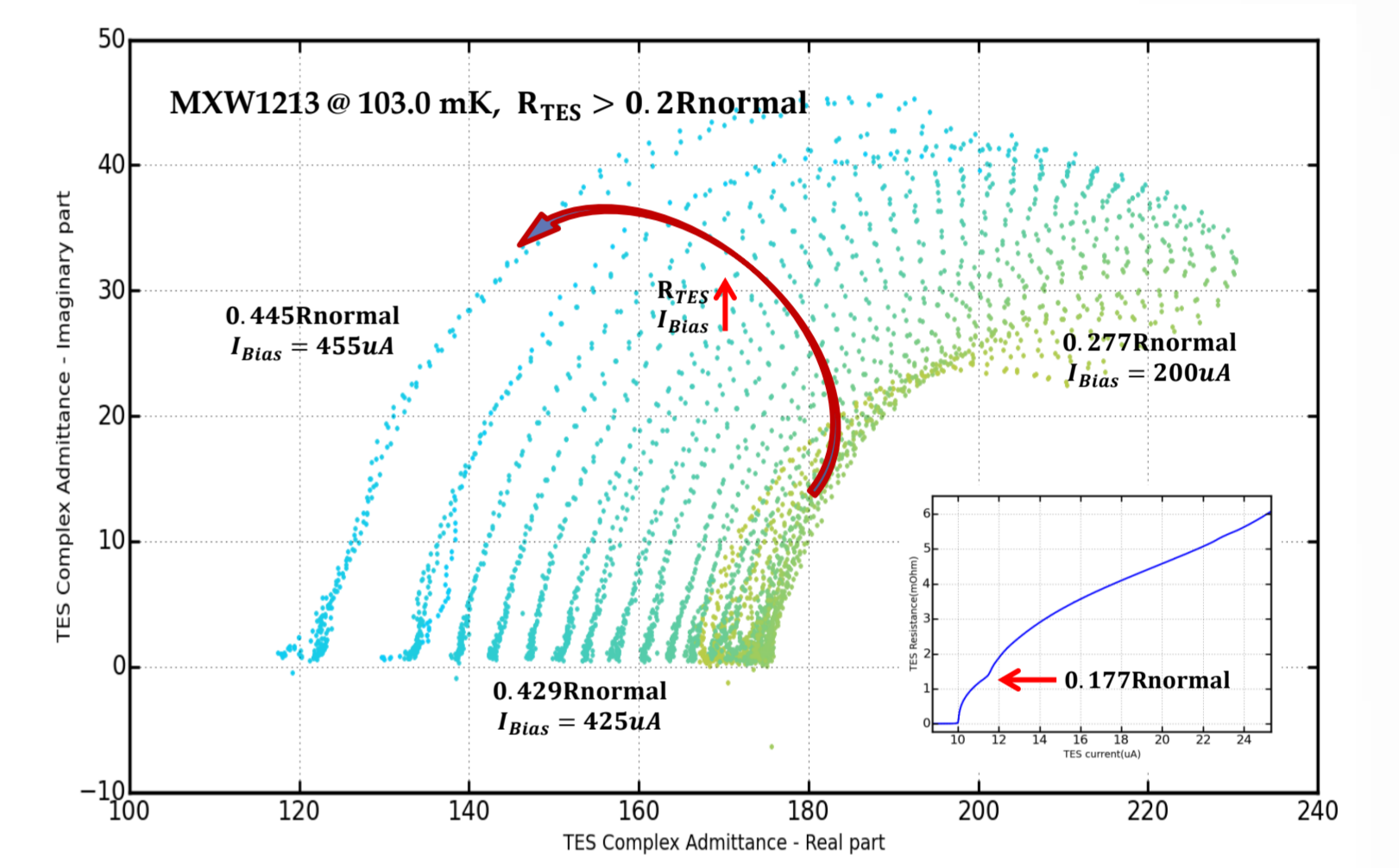
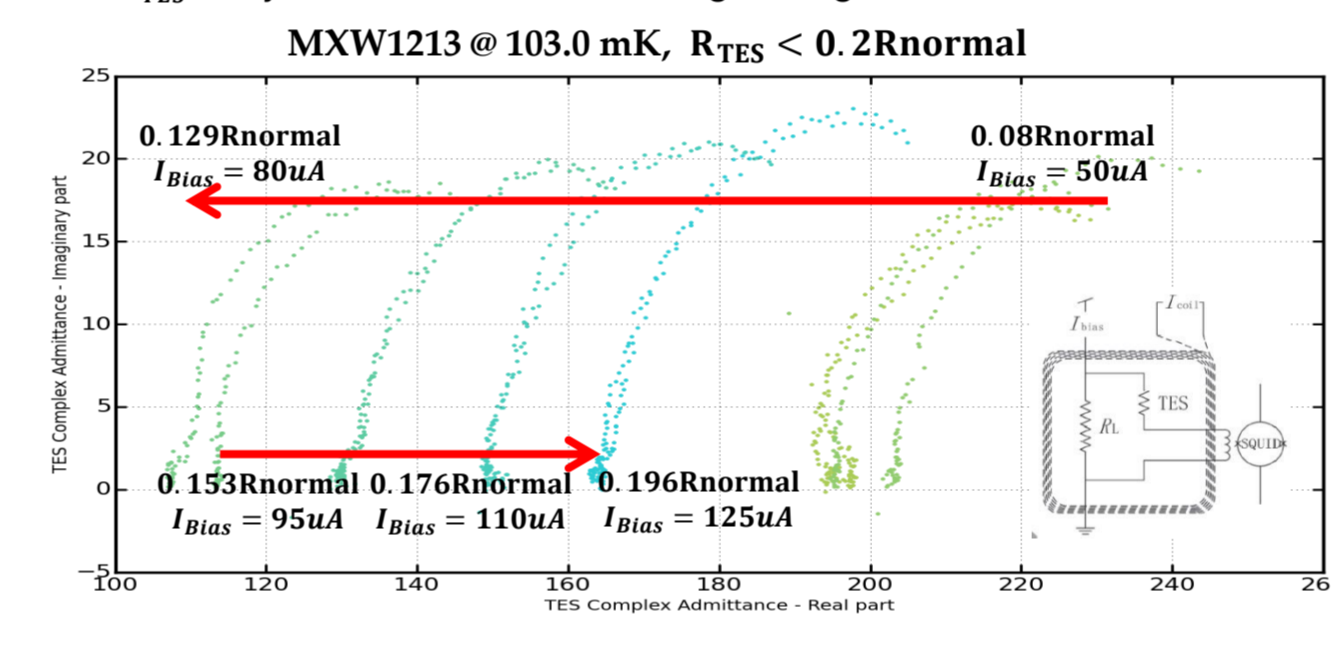
$$\beta = \frac{\partial \ln R}{\partial \ln I}$$



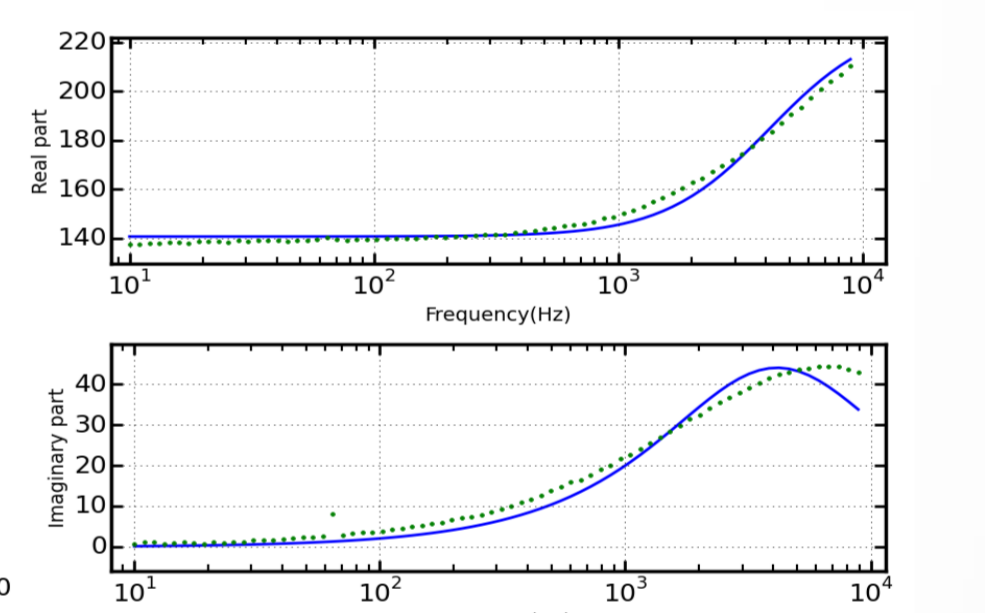
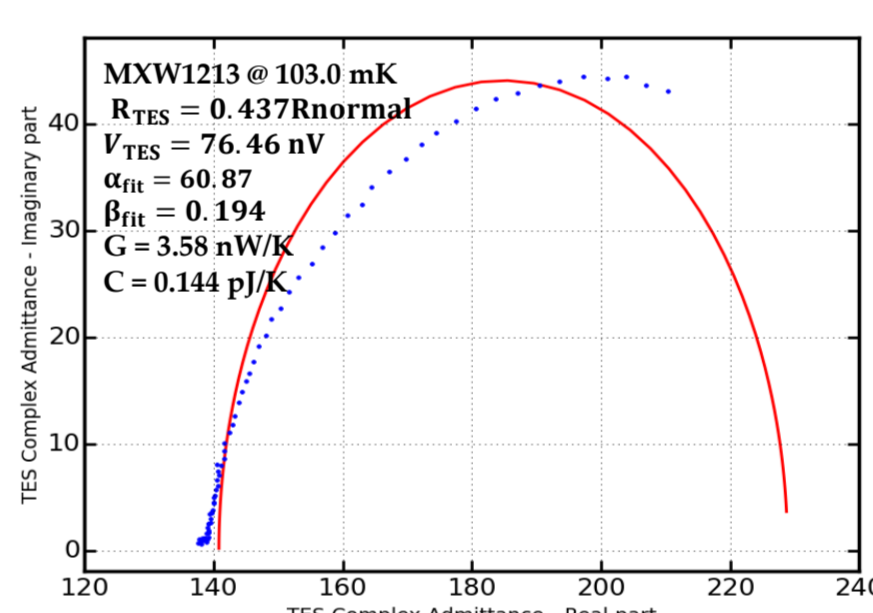
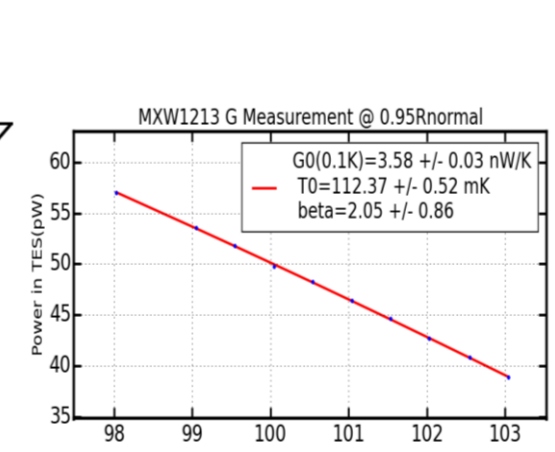
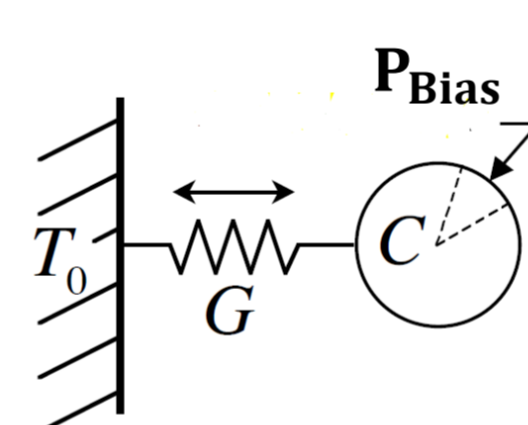
Complex Admittance Evolution

At 103.0mK base temperature the TES complex admittance calculated using an empirical Thevenin equivalent circuit for the bias and SQUID network [3] is driven by the bias current.

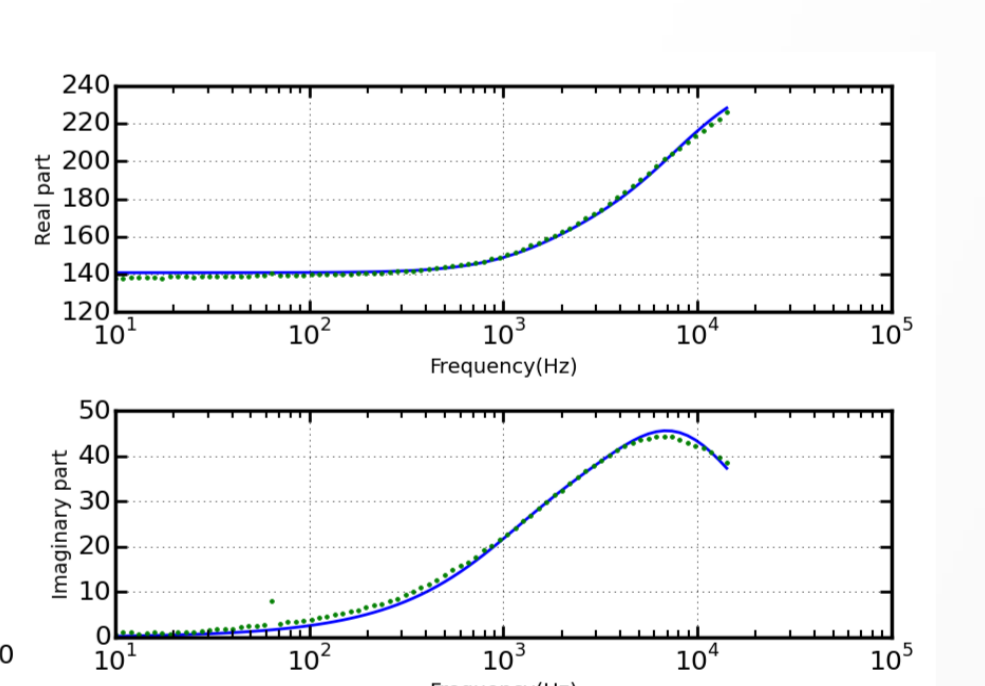
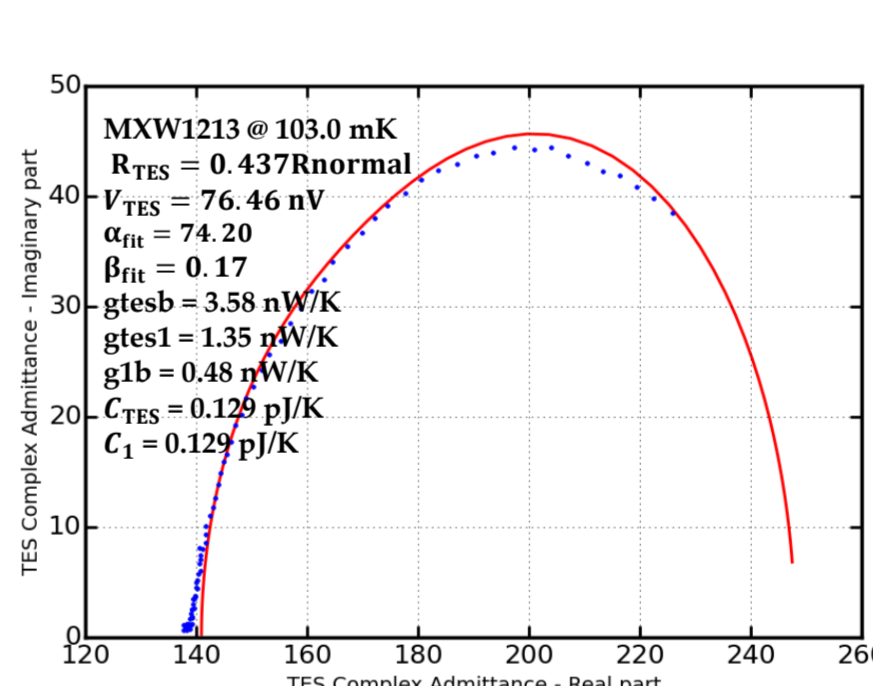
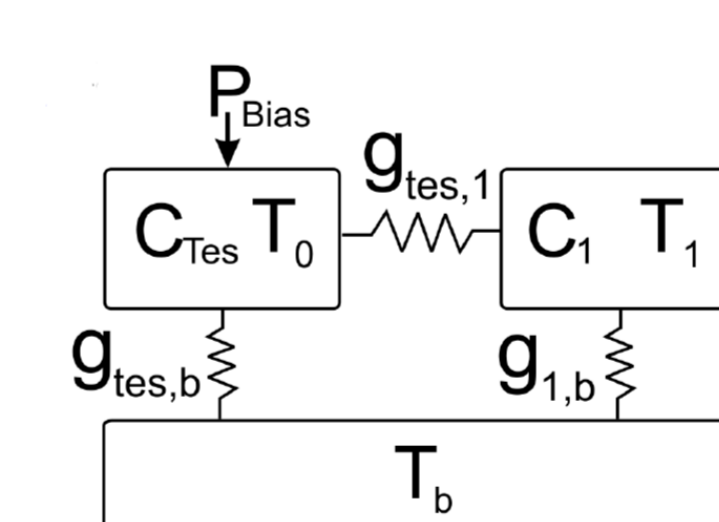
Starting from the right side, the admittance jumps to the very left side and then moves toward the right while its size roughly stays constant when R_{TES} < 0.2R_{normal}. After R_{TES} is beyond 0.2R_{normal}, it starts to grow larger and move to the left.



Thermal model 1[1]

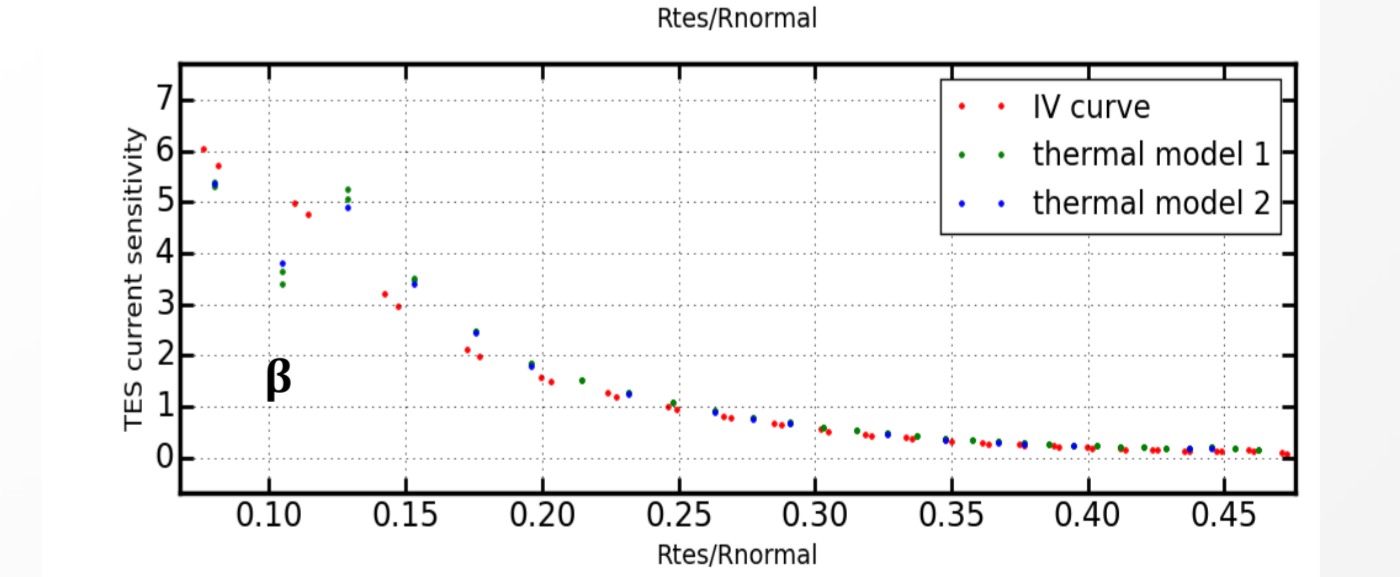
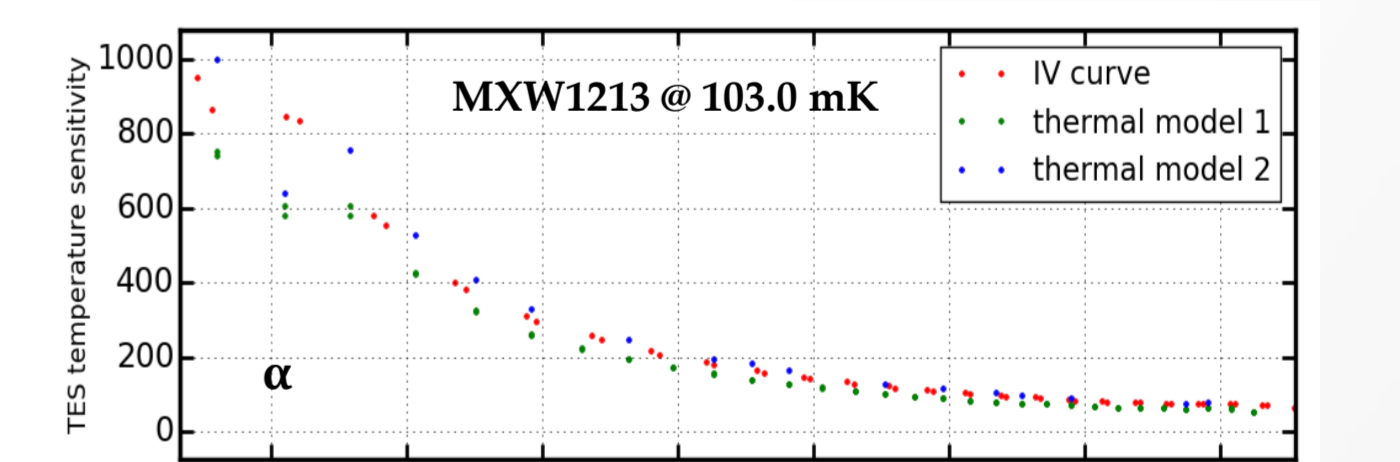
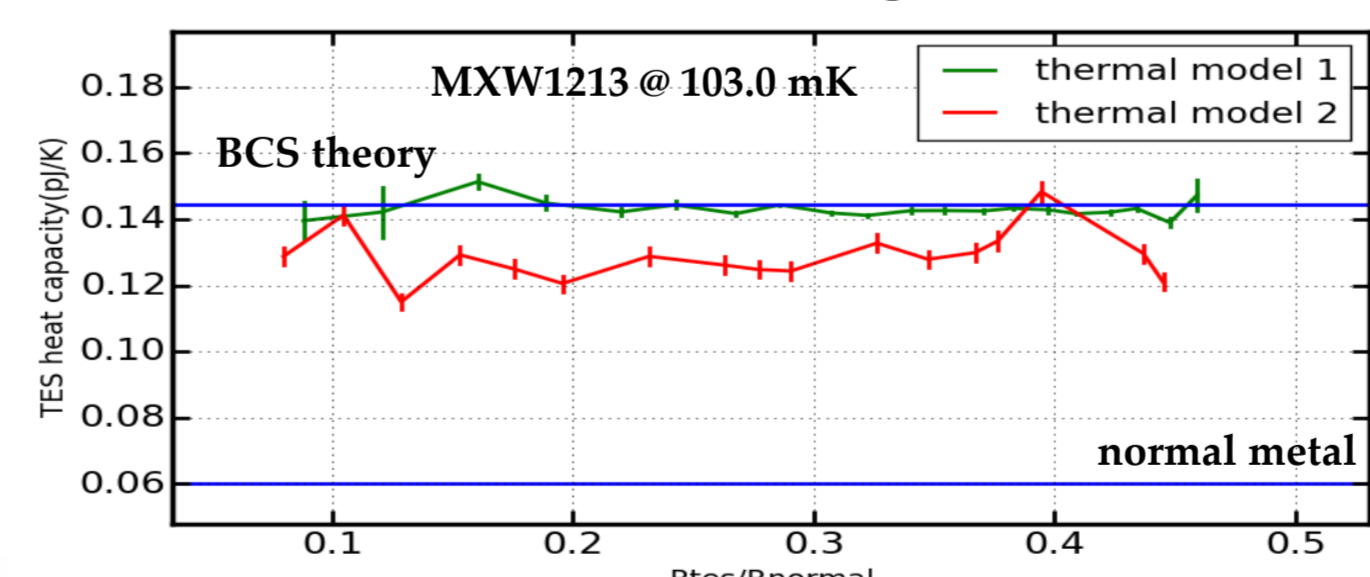


Thermal model 2[2]



Compare α & β from IV curve with complex admittance fitting result

Heat capacity through transition



References

1. McCammon, Dan. "Thermal equilibrium calorimeters—an introduction." *Cryogenic particle detection* (2005): 1-34.
2. Maasilta, Ilari J. "Complex impedance, responsivity and noise of transition-edge sensors: Analytical solutions for two-and three-block thermal models." *Aip Advances* 2.4 (2012): 042110.
3. Lindeman, M. A., et al. "Accurate thermal conductance and impedance measurements of transition edge sensors." *Journal of Low Temperature Physics* 151.1-2 (2008): 180-184.
4. Zhang, Shuo, et al. "Mapping of the resistance of a superconducting transition edge sensor as a function of temperature, current, and applied magnetic field." *Journal of Applied Physics* 121.7 (2017): 074503.
5. K. M. Morgan, S. E. Busch, M. E. Eckart, C. A. Kilbourne, D. McCammon, "Large Area Transition Edge Sensor X-ray Microcalorimeters for Diffuse X-ray Background Studies", *JLTP* 176, 331 (2013)
6. Jethava, Nikhil, et al. "Dependence of excess noise on the partial derivatives of resistance in superconducting transition edge sensors." *AIP Conference Proceedings*. Vol. 1185. No. 1. AIP, 2009.
7. J. Sadleir, Applied Superconductivity Conference, 2016
8. S. Shapiro, "Josephson currents in superconducting tunneling: The effect of microwaves and other observations" *Physical Review Letters* 11, 80 (1963). C. C. Grimes and S. Shapiro, *Physical Review* 169, 397 (1968).

Contact Information:

zhou326@wisc.edu ; zhouyu14@mails.tsinghua.edu.cn

Summary

1. We characterized two TES devices and compared them. The TES with no finger or bank structures is more sensitive to the magnetic field than the three finger TES, while the period of the fringes on the BI curve is about the same for both devices.
2. The IV curves of both devices show Shapiro steps when a high frequency external field is applied. More Shapiro steps are visible on the zero finger TES IV curve than the three finger TES.
3. The simple thermal model with only one time constant can't fit the complex admittance very well. The fitting results give smaller α compared with IV curve. The two block thermal model yields a better fit.